SANJA GRUBEŠA, B.Eng.El.
E-mail: sanja.grubesa@fer.hr
HRVOJE DOMITROVIĆ, Ph.D.
E-mail: hrvoje.domitrovic@fer.hr
KRISTIAN JAMBROŠIĆ, Ph.D.
E-mail: kristian.jambrosic@fer.hr
University of Zagreb,
Faculty of Electrical Engineering and Computing
Unska 3, HR-10000 Zagreb, Croatia

Traffic and Environment (Ecology)
Original Scientific Paper
Accepted: Dec. 17, 2010
Approved: May 17, 2011

PERFORMANCE OF TRAFFIC NOISE BARRIERS WITH VARYING CROSS-SECTION

ABSTRACT

The efficiency of noise barriers largely depends on their geometry. In this paper, the performance of noise barriers was simulated using the numerical Boundary Element Method (BEM). Traffic noise was particularly considered with its standardized noise spectrum adapted to human hearing. The cross-section of the barriers was varied with the goal of finding the optimum shape in comparison to classical rectangular barriers. The barrier performance was calculated at different receiver points for a fixed barrier height and source position. The magnitude of the insertion loss parameter was used to evaluate the performance change, both in one-third octave bands and as the broadband mean insertion loss value. The proposed barriers of varying cross-section were also compared with a typical T-shape barrier of the same height.

KEY WORDS

traffic noise, noise barriers, noise reduction

1. INTRODUCTION

The ever-growing movement of both people and goods brings as a consequence the permanent growth of all kinds of traffic. Therefore, traffic noise (including road, railway, air and ship traffic) is the most important issue when considering the size of areas where noise values exceed the limits stipulated by legislative documents, as well as the number of people affected by those excessive values [1]. When designing new traffic routes, it is possible to reduce the impact of noise on people and the environment by choosing traffic routes outside inhabited places and by integrating them into the existing terrain relief. On the other hand, the noise abatement solutions for existing traffic routes are mainly directed towards the design of noise barriers. Their efficiency depends on design parameters.

It is well known that the efficiency of a noise barrier is conditioned by its position and its geometry, height being the most important parameter [2]. It is not practical to build very high barriers for aesthetical and practical reasons. In order to increase their efficiency, new types of barriers of different shapes have to be devised with respect to the requirement that the height should be kept in reasonable limits, but still ensuring enough noise level reduction. The increase of barrier height is directly followed by the increase in its price. Moreover, there is another major construction problem – the designed barrier, when assembled, has to maintain its required mechanical stability. The problem of maintaining reasonable barrier height can be solved by adding an element to the top of the barrier acting like a sound diffuser. Following this procedure yields different barrier shapes, such as flat-top, round-top, Y, T barriers, etc.

A number of authors tried to solve the problem of the optimal barrier shape using experimental or numerical approach. For barriers with a complex shape, where no analytical method can be used, Seznec [3] proposed the development of a program that uses numerical calculation with boundary elements (Boundary Element Method, BEM). Hothersall et al. [4, 5] studied a number of barriers by comparing the plain barrier with barriers that had a special circular, Y- or T-shaped element installed on the top. The Y- and T-shaped elements have proven to work very well for sound diffusion. The T shape was further studied by Baulac et al. [6], as well as Monazam and Lam [7], and a contribution to the optimization of Y shaped barriers was given by Grainer et al. [8]. Ishizuka and Fujiware [9] compared the efficiency of a number of different types of diffusers placed on top of the barriers. Crombie et al. [10] used numerical calculations as well as physical models of noise barriers in order to study the function of multiple barriers, one behind the other. They showed that with multiple barriers better noise protection is obtained compared to a single barrier. Similar

conclusions were made by Martin and Hothersall [11] using additional median road traffic noise barriers. Furthermore, in their numerical calculations some authors considered barriers whose parts, usually the top diffusers, were made of sound absorbing materials. The acoustic impedance of those materials is finite, compared to the simplified approach of modelling in which the barriers are assumed to have totally reflecting surfaces of infinitely large impedance. In practical design, infinite impedance of a barrier surface relates to using acoustically very reflective materials such as reinforced concrete. Lim et al. [12] considered in detail the differences in barrier efficiency related to acoustic impedance of materials used to construct the top diffusers.

Previous research rarely considered the influence of a barrier cross-section shape on its efficiency because barriers with parallel and flat surfaces have been usually designed. If an increase of barrier efficiency is investigated, it is always achieved by adding diffusers to its top. Placing the diffusers on top of barriers is always connected with the increase of barrier construction expenses, especially if these diffusers are built from sound absorbing materials. The justification of the barrier price increase is found in the higher barrier efficiency, or in other words, in the lower noise imission levels which is characterized by the rise of the insertion loss parameter.

The materials a barrier is made of have to have a sufficiently large index of sound insulation so that the dominant part of noise at the imission location originates from the sound being diffracted over the top of the barrier, and not from the sound penetrating through it. For a properly designed barrier, the level of noise part penetrating through the barrier has to be at least 10dB lower than the level of noise diffracted over it. The optimal values of this level difference exceed 20dB.

In this paper, the influence of barrier cross-section on barrier efficiency is considered using the boundary element method. The goal of the research is to find the most efficient shape of the barrier cross-section which would at the same time be simple enough for practical design and assembly.

2. MODELLING OF THE SOUND SOURCE

For use in numerical calculations, the majority of real sound sources can be represented as point or line sources, regardless of their size or shape. Sound propagates from a point source equally in all directions, thus producing a spherical wave. If we observe the surface through which the sound energy passes, the sound pressure of an ideal point source at some observation point is inversely proportional to the distance r between the source and the observation point. In reality, there is no ideal point source. Therefore, in order to define the parameters on which the sound pressure of a real source depends, first we have to define the near (Fresnel) and the far (Fraunhofer) zone. The boundary between these zones depends on the physical size of the source as well as on the frequency of the sound waves emitted by the source.

The sound pressure p of a planar circular source shown in *Figure 1* is defined by (1), where a is the source radius, k is the wave number ($k = 2\pi/\lambda$), ω is the circular frequency, λ is the wavelength of the emitted sound wave, $\rho_0 c$ is the acoustic impedance of the medium, and U_0 is the surface velocity of the source.

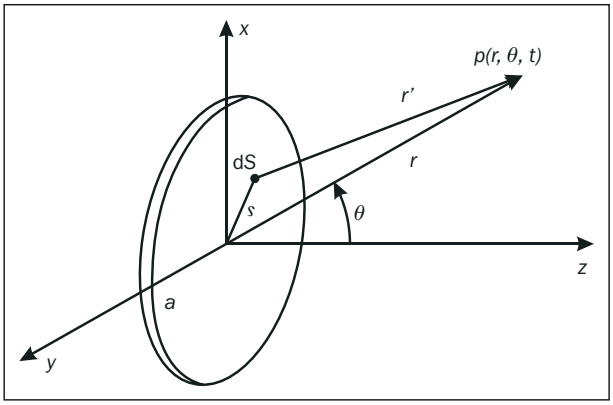

Figure 1 – A circular sound source [13]

$$p(r,\theta,t) = j\rho_0 c \frac{U_0}{\lambda} \int_S \frac{1}{r} e^{j(\omega t - kr')} dS \qquad (1)$$

The broken line in *Figure 2* shows the Fraunhofer approximation of the normalized sound pressure for the far field, and the solid line was obtained by the extrapolation of the Fraunhofer approximation of the normalized sound pressure to the Fresnel zone. The boundary between the Fresnel and Fraunhofer zone can be marked as r_1 which has a physical meaning only if the ratio a/λ is large enough in order that $r_1 > 0$. If $a = \lambda/2$, then $r_1 = 0$ and there is no Fresnel zone, i.e. there is no interference and the sound source can be represented as an ideal point source. When $r > r_1$, the sound pressure magnitude falls continuously and

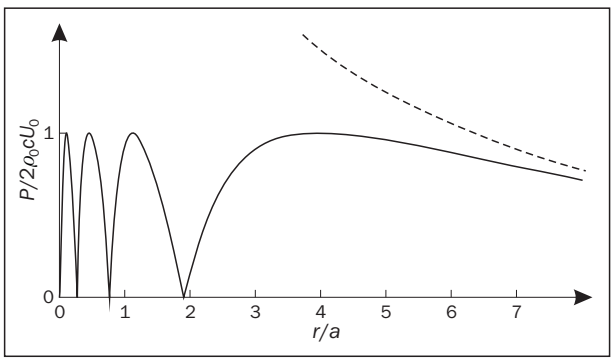

Figure 2 - Normalized sound pressure for a circular sound source, [13]

asymptotically approaches the $1/r$ curve, while for $r < r_1$ the amplitude shows interfering behaviour.

The sound pressure magnitude $p(r,\theta)$ of a line source of finite length L and radius a shown in *Figure 3* is defined by (2), where $p_{ax}(r)$ represents the magnitude proportional with $1/r$ in the far field (3), and $H(\theta)$ is the directivity factor which depends on the sync function or the spherical Bessel function (J_0) of zero order, as in (4).

$$p(r,\theta) = p_{ax}(r) \cdot H(\theta) \tag{2}$$

$$p_{ax}(r) = \frac{1}{2}\rho_0 c U_0 \frac{a}{r} kL \tag{3}$$

$$H(\theta) = \frac{\sin(\nu)}{\nu},\ \nu = \frac{1}{2}kL\sin(\theta) \tag{4}$$

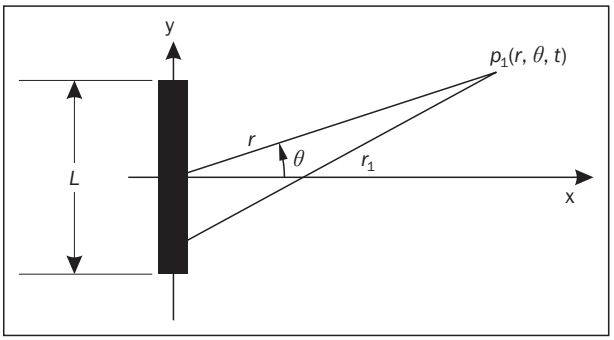

Figure 3 - A line source of finite length, [13]

Figure 4 shows the directivity factor $H(\theta)$ for a line source of finite length, with the parameter $kL = 24$. The directivity factor is directly responsible for the appearance of side lobes, i.e. for the sound dispersion. Different sound sources have different directivity factors. It can be shown that the sound pressure magnitude in the Fraunhofer zone for a line source behaves in the same way as for a point source and a plane circular source, i.e. it decreases proportional to $1/r$. In the Fresnel zone, there is a different situation: when $r >> \lambda$, the sound pressure magnitude falls according to $1/\sqrt{r}$.

In numerical calculations of the sound field using the boundary element method, a simplified model of

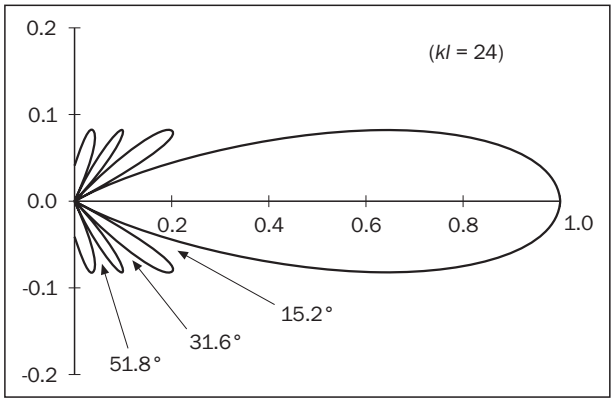

Figure 4 - Directivity factor for a line source of finite length, [13]

the traffic road is usually used. It is represented by a line source of infinite length. In this case, the directivity factor of the line source is constant for all points with the same distance from the source axis. The sound field has a cylindrical shape, i.e. the sound spreads equally all around the road axis, with a decrease of sound pressure proportional to $1/r$. This simplification is very often used in such models because there are no significant discrepancies to real measurements if the traffic is dense enough, as shown in Jean et al. [14].

3. SOUND PRESSURE CALCULATION USING BEM

There are a lot of empirical expressions that define the traffic noise levels at the imission point. These expressions are used in various numerical models integrated into numerous international and national standards and regulations. The analytical expressions are of limited accuracy because they do not take into account the precise configuration of the terrain and all other obstacles to the free field sound propagation [15].

One of the main numerical tasks that have to be solved while determining the noise levels in some area is to know how much a certain noise barrier reduces noise levels. If we assume that the sound pressure in each point of space depends harmonically on time, then the sound pressure is given by (5), where x, y and z are Cartesian coordinates of the imission point. In order to obtain the sound pressure value in that point, a solution to the homogenous Helmholtz equation given by (6) has to be found, where $k = \omega c = 2\pi/\lambda$ is the wave number (rad/m), c is the speed of sound (m/s), λ is the wavelength (m). If there is a source in position (x_0,y_0,z_0), the sound field can be described by a homogenous Helmholtz equation (7), where $\delta(x-x_0,y-y_0,z-z_0)$ is the spatial Dirac function. For this function, expression (8) can be written.

$$P(x,y,z,t) = p(x,y,z,t) \cdot e^{j\omega t} \tag{5}$$

$$\nabla^2 p(x,y,z) + k^2 p(x,y,z) = 0 \tag{6}$$

$$\nabla^2 p(x,y,z) + k^2 p(x,y,z) = \\ = -4\pi A\delta(x-x_0,y-y_0,z-z_0) \tag{7}$$

$$\iiint_V \delta(x-x_0,y-y_0,z-z_0)\mathrm{d}V = 1 \tag{8}$$

The sound pressure p_s of a spherical wave is given by expression (9). It represents the solution of equation (7), its magnitude equals A/r (Pa/m). The magnitude decreases with factor $1/r$ where r represents the distance between the source and the imission point, and is given by expression (10).

$$p_s = \frac{A \cdot e^{jkr}}{r} \tag{9}$$

$$r = \sqrt{(x - x_0)^2 + (y - y_0)^2 + (z - z_0)^2} \quad (10)$$

The boundary element method (BEM) is a well known numerical method for obtaining approximate solutions to the boundary integral equations, particularly the fore mentioned Helmholtz integral equation. Although it has been known for decades, it became more popular only recently with the increase of computer computational power. The BEM method is based on discretization of the integral equation which represents the equivalent of the original partial differential equation, Kirkup and Yazdani [16].

The insertion loss of noise barriers with complex shapes cannot be calculated using simple analytical equations. The BEM method is often used to calculate the acoustic efficiency of noise barriers with arbitrary shapes and surface acoustic impedances. Therefore, the open source Matlab routine toolbox OPENBEM [17] was used for the calculations in this paper. The 2D module of this toolbox enables the calculation of the sound pressure levels in an open half-space with a defined sound source position and barrier shape.

4. SIMULATION PARAMETERS

If the noise of road traffic is investigated, the normalized traffic noise spectrum in one-third octave frequency bands is usually used for determining the efficiency of noise barriers, *Table 1* [18]. The table shows that the majority of the traffic noise energy is located in the frequency range around 1kHz, which corresponds to the frequency range where human hearing shows the highest sensitivity. It is obvious that traffic noise components with frequencies between 500Hz and 2kHz are the ones that determine the total level of the traffic noise. Therefore, the efficiency of the barriers has to be optimized for this frequency range. On the other hand, one of the goals of the car designing process is to reduce the traffic noise level and change its frequency spectrum in order to be more acceptable [19, 20]. Nevertheless, using the normalized levels of traffic noise enables a good estimation of noise barriers efficiency.

A noise barrier can be defined as a non-transparent obstacle to sound propagation between the sound source and the listener, where the noise propagates either above or around the barrier. The sound level will decrease at the receiving point compared to the source location because of the distance over which the sound propagates between these two points, but additionally also because of the construction of the noise barrier as a sound propagation obstacle. The decrease of the sound level achieved by the insertion of the sound barrier is called the insertion loss. The insertion loss *IL* is usually used as a measure for comparing the efficiency of various noise barriers. It is defined as the difference of sound pressure level p_p measured at the receiver point before the noise barrier has been installed and sound pressure p_n measured after installation. It is assumed that no changes have been made in the configuration of the terrain or the position of the noise source and the receiving point (11).

$$IL = 20 \log\left(\frac{p_p}{p_n}\right) \quad (11)$$

The efficiency of a noise barrier directly depends on the frequency of the sound wave which propagates over it. Therefore, the insertion loss is highly frequency dependent. For this reason, the mean insertion loss parameter is introduced. It is defined as a broadband reduction in noise levels before and after installing a noise barrier for the one-third octave band frequencies in the range where barrier efficiency is important, i.e. from 100 to 4,000Hz.

5. NOISE BARRIER MODELS

This investigation has considered the barriers that have flat surfaces inclined towards the noise source, i.e. the road. The inclination angle of the surfaces depends on the number of inclined sections, barriers type 2, 3 and 4 in *Figure 5*. The surface of the barrier facing away from the noise source remains perpendicular to the ground. Therefore, the cross section of the proposed noise barrier models changes with height. The barrier of type 1, a plain reference barrier of the same height (4m) and minimum depth (0.2m) was used for comparison with the proposed barriers of types 2-4. Type 5 barrier with the T-shaped diffuser on top, centred over the barrier base was also used for comparison. This barrier was chosen for efficiency comparison because it is used very often in real life applications. The top section is 1m wide, unlike barrier types 2-4 with the top width of 0.5m, or the reference barrier type 1 with top width of 0.2m.

Figure 6 shows the 2D representation of the simulated terrain configuration used for the numerical calculation of noise barrier efficiency. The location of the sound source S, the barrier B and the receiving points R1, R2 and R3 were chosen based on typical real-life values. The typical distance between the noise source (representing the median line of the traffic road) and the barrier is 4m, the source height is 0.5m representing the height of the engines in the vehicles passing

Table 1 - Normalized levels of road traffic noise L_i for one-third octave frequency bands

f_i (Hz)	100	125	160	200	250	315	400	500	630	800	1,000	1,250	1,600	2,000	2,500	3,150	4,000	5,000
L_i (dB)	-20	-20	-18	-16	-15	-14	-13	-12	-11	-9	-8	-9	-10	-11	-13	-15	-16	-18

by, the typical barrier height is 4m, and the typical listener ear height at the receiving points while the listener is standing equals 1.5m. The receiving points are positioned at 10, 20 and 50m distance from the barrier, respectively.

The ground and all barrier types were simulated as reflective surfaces with infinite acoustic impedance which is an often used approximation of the outdoor sound field environment.

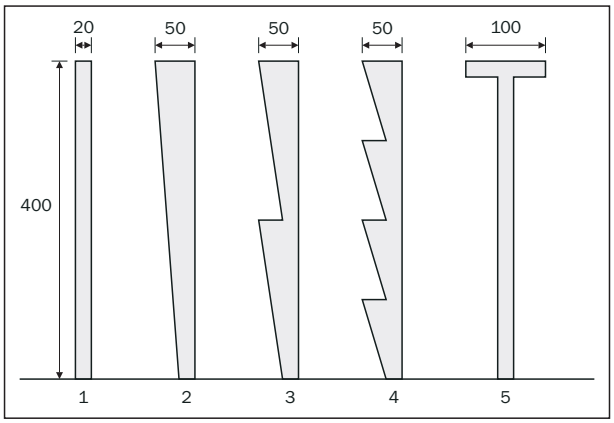

Figure 5 - Cross-section of barrier types used in this paper: type 1 – reference plain barrier, types 2 to 4 – proposed barriers with variable cross-section, 5 – T barrier for comparison

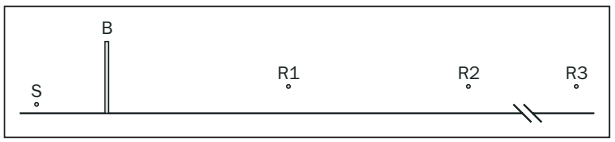

Figure 6 - Simulated terrain configuration with indicated positions of the noise source (S), the barrier (B) and the receiving points (R1 – R3).

6. SIMULATION RESULTS

As BEM solves the integral equation of the sound wave at a certain frequency in order to calculate the sound levels in the defined area, certain frequencies have to be chosen which would represent the behaviour of the barrier in the whole frequency range of interest. All numerical calculations were done for frequencies corresponding to the centre frequencies of one-third octave bands.

The source emission levels were calibrated to the normalized levels as shown in *Table 1*. As the source and the receiving points are located near a hard reflecting surface (the terrain plane), it was necessary to control the sound levels at the receiving points in the simulation environment. *Figure 7* shows the spectra of the noise sound pressure level (SPL) at all three receiving points for the case when there is no barrier in the simulation. Although it can be seen that the noise levels fall within the distance as expected, there is also a minimum in the levels at different frequencies for different receiving points as the consequence of the addition of the direct wave coming from the sound source, and the wave reflected from the ground surface of infinite impedance. Thus, the spectra represent the usual "comb-filter" effect. Only at the farthest point R3 the minimum moves to higher frequencies and the shape of the spectrum starts to look similar to the normalized traffic spectrum from *Table 1*. Nevertheless, it is evident that the majority of sound energy of the traffic noise is located in the middle frequency range at all receiving points.

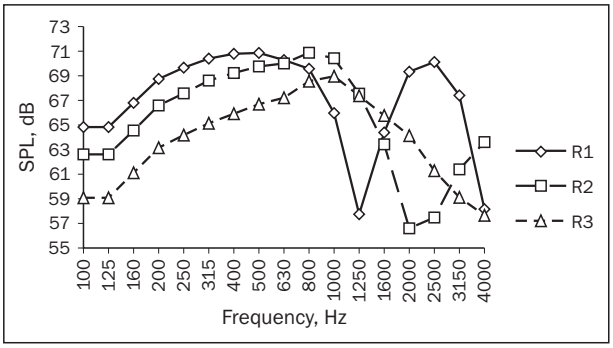

Figure 7 - Noise spectra at the receiving points R1, R2 and R3 with no barrier placed between the source and the receiving points

Figures 8, 9 and 10 show the insertion loss parameter for all simulated barriers in one-third octave frequency bands, at receiving points R1, R2 and R3, respectively. All simulated barrier types were designed as totally reflective.

The results show that the three new proposed barrier types (2, 3, and 4) have higher values of insertion loss in the whole frequency region with respect to barrier type 1, with the most significant improvement in the frequency region around 2,000Hz. Type 2 barrier exhibits the highest insertion loss in the frequency region of interest (500Hz to 2,000Hz).

The addition of absorptive materials on the barrier surface in the simulation did not improve the insertion loss, and in reality it would only increase the production costs.

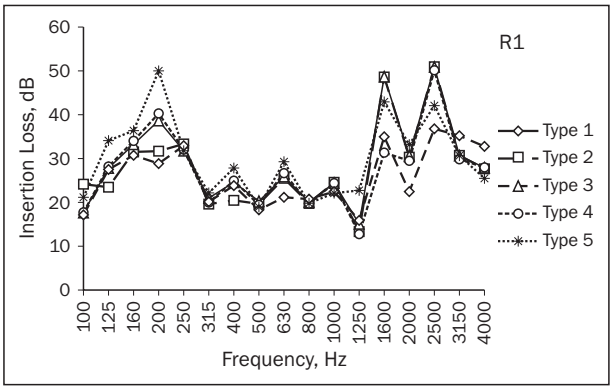

Figure 8 - Insertion loss for all barrier types in one-third octave bands from 100 to 4,000Hz at receiving point R1

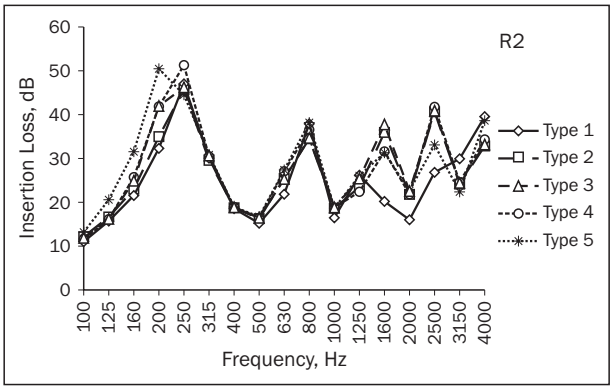

Figure 9 - Insertion loss for all barrier types in one-third octave bands from 100 to 4,000Hz at receiving point R2

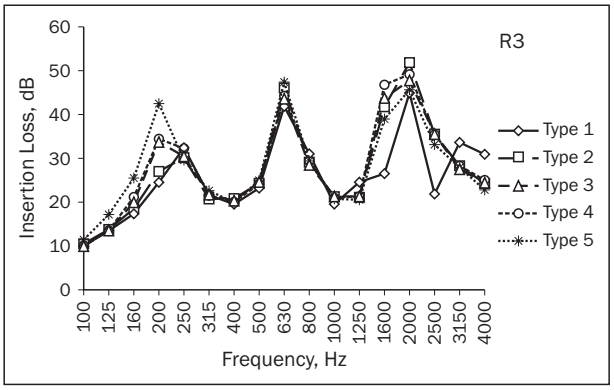

Figure 10 - Insertion loss for all barrier types in one-third octave bands from 100 to 4,000Hz at receiving point R3

Figure 11 shows the values of mean insertion loss for all five simulated barrier types, depending on the distance between the barrier and the receiving point. It can be seen that a plain type 1 barrier has the lowest mean insertion loss, while the T barrier exhibits the highest value of this parameter. The three proposed barriers have approximately the same mean insertion loss values, which are about 1.5dB better than the reference barrier, but still about 1dB lower than the value obtained for a T-shaped barrier. The difference between the mean insertion loss of barrier types 2, 3, 4 and 5 compared to the values calculated for the reference barrier type 1 are given in *Table 2*. The improvement in the insertion loss averaged over all three receiving points is between 1 and 1.5dB, depending on the barrier type. The chart shows that the most effective type of barrier out of the ones proposed in this investigation is type 4. The increase in sound insertion loss obtained with barrier type 4 can also be achieved by enlarging the effective height of the reference plain barrier (type 1) by 0.9m, as shown in *Table 2*.

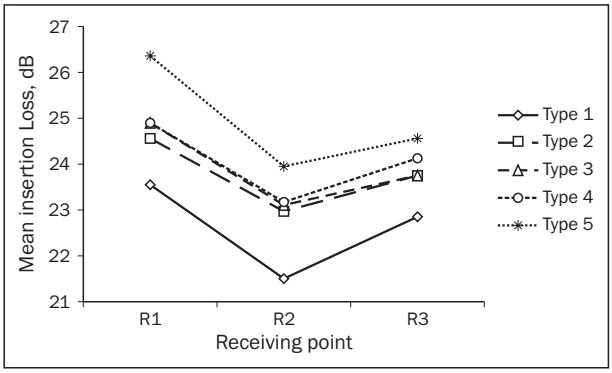

Figure 11 - Mean insertion loss for all 5 simulated barrier types depending on the receiving point

Table 2 - Mean insertion loss differences between barrier types 2-5 and the reference barrier type 1 at receiving points R1, R2 and R3. In the last row – mean IL difference between a plain barrier of 4.9 m height (type 1 with increased height), and the reference barrier

Barrier type	Mean IL difference			
	R1	R2	R3	Average
2	1.02	1.47	0.89	1.13
3	1.32	1.54	0.89	1.25
4	1.36	1.66	1.27	1.43
5	2.81	2.46	1.69	2.32
1'	0.11	2.09	1.90	1.37

In order to have a better understanding of barrier efficiency observed over an area rather than on discrete receiving points, a graphical representation of sound levels calculated for a receiving point grid is common. The grid spacing depends on the emitting frequency of the sound source, with a minimum of six grid points per wavelength.

Figure 12 shows a calculation example for type 2 barrier at 500Hz. In the top picture the absolute sound pressure level can be seen, and in the bottom part the difference between the free field sound pressure level and the levels calculated with the inserted barrier. Because of the interfering character of the sound field at a single frequency due to sound reflection and diffraction, the bottom representation shows the actual improvement with the addition of a barrier. The darker shades of grey show a bigger difference in the sound levels compared to the free field condition.

Another calculation example is shown in Figures 13 and 14. They show the comparison between the barriers of type 1 and type 2 at frequency 1,600Hz, i.e. the difference of the calculated sound pressure levels with the barrier and in free field conditions, as shown in *Figure 12*, bottom part. It is obvious that there are darker areas for barrier type 2 at its right side compared to barrier type 1, which is a measure of the improved barrier's efficiency.

7. CONCLUSIONS

The primary goal of traffic system technologies is to enable the transportation of people and goods. Nevertheless, while planning and designing new and

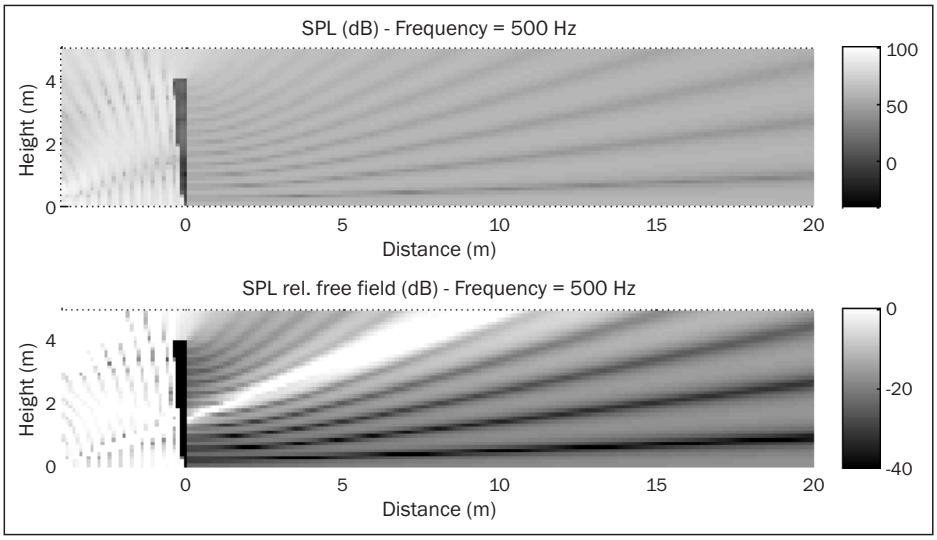

Figure 12 - Calculation example for barrier type 2 at 500Hz. Top – the calculated sound pressure level at the receiving grid. Bottom – the difference in sound pressure level between the calculated values from the top picture and the free field sound pressure levels

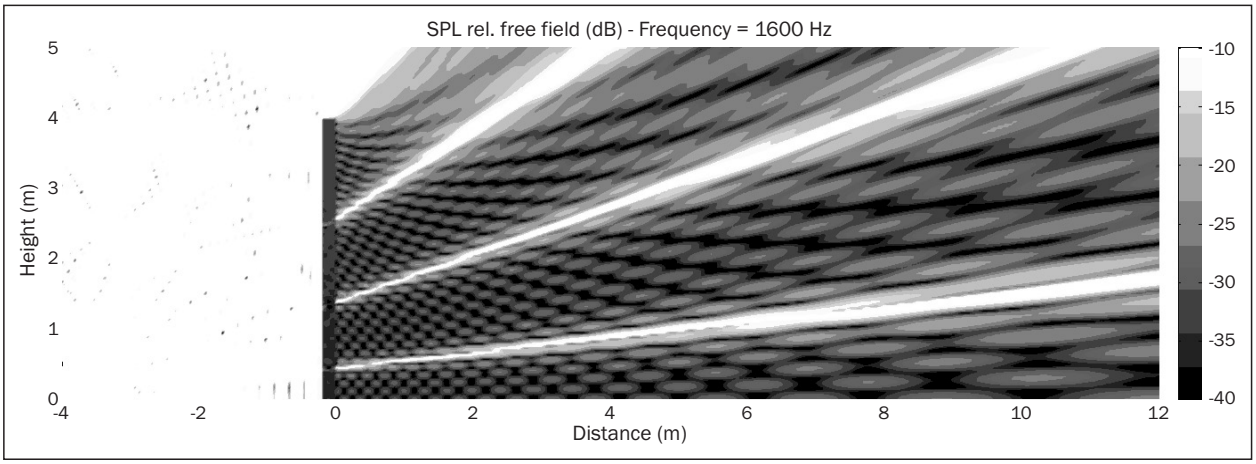

Figure 13 - Sound pressure level differences when inserting barrier type 1 at 1,600Hz

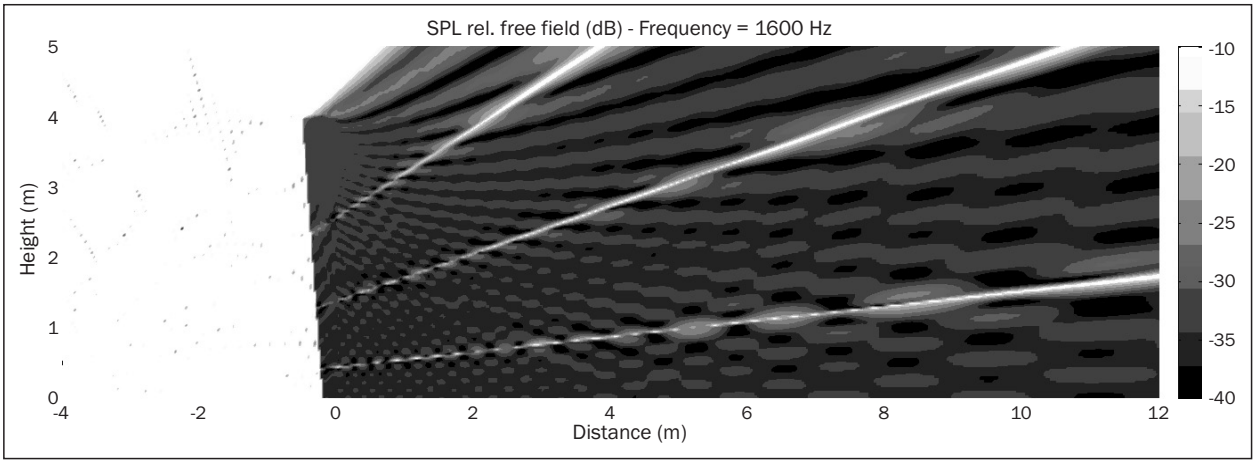

Figure 14 - Sound pressure level differences when inserting barrier type 2 at 1,600Hz

analysing the existing systems, their impact on the environment has to be considered. This paper studies the improvement of noise barrier efficiency, where barriers are considered as the building elements of traffic systems which reduce the traffic noise influence on people and the environment. The improvement was analyzed through the increase of sound insertion loss. The vertical barrier cross-section varied while keeping

constant height for all barrier types. The results obtained using the BEM calculation method showed an increase in sound insertion loss up to 1.5dB compared to a reference plain barrier of the same height and width. The proposed barrier shapes evidently bring a saving in barrier height and reduce the construction costs, at the same time enabling easier visual integration of the barrier into the surroundings. At the same time, it is important to select a solid material with less density than concrete to build such a barrier because of the stability and construction problems. Lightweight structure filled with sand could be a practical option.

SANJA GRUBEŠA, dipl. ing. el.
E-mail: sanja.grubesa@fer.hr
Dr. sc. **HRVOJE DOMITROVIĆ**
E-mail: hrvoje.domitrovic@fer.hr
Dr. sc. **KRISTIAN JAMBROŠIĆ**
E-mail: kristian.jambrosic@fer.hr
Sveučilište u Zagrebu, Fakultet računarstva i elektrotehnike
Unska 3, 10000 Zagreb, Hrvatska

SAŽETAK

KARAKTERISTIKE PROMETNIH BUKOBRANA S PROMJENJIVIM POPREČNIM PRESJEKOM

Učinkovitost bukobrana u najvećoj mjeri ovisi o njihovoj geometriji. U ovom radu su simulirane karakteristike bukobrana metodom rubnih elemenata (eng. Boundary Elementh Method). Korištena je buka prometa sa svojim normiranim spektrom koji je prilagođen ljudskom sluhu. Poprečni presjek bukobrana mijenjan je s ciljem pronalaska optimalnog oblika u usporedbi s klasičnim ravnim bukobranima. Karakteristike bukobrana su proračunavane za različite pozicije prijamnika uz definirane visine bukobrana i poziciju izvora. Za ocjenu promjene učinkovitosti upotrijebljen je parametar smanjenja buke uslijed postavljanja bukobrana (eng. Insertion Loss), i to u tercnim frekvencijskim pojasevima te kao širokopojasna jednobrojčana vrijednost. Predloženi bukobrani s promjenjivim poprečnim presjekom također su uspoređeni s tipičnim bukobranom T oblika iste visine.

KLJUČNE RIJEČI

buka prometa, bukobrani, smanjenje buke

LITERATURE

[1] **Sviben, Z.**, **Toš, Z.**: *Some Aspects of Pollution and Noise in Zagreb City Traffic Preliminary Communication*, Promet Traffic&Transportation, Vol. 13, 2001, pp. 115-118

[2] **Bies, D. A.**, **Hansen, C. H.**: *Engineering Noise Control, Theory and Practice*, Spon Press, 2009

[3] **Seznec, R.**: *Diffraction of sound around barriers: use of the boundary elements technique*, Journal of Sound and Vibration, Vol. 73, 1980, pp. 195–209

[4] **Hothersall, D.C.**, **Chandler-Wilde, S.N.**, **Hajmirzae, M.N.**: *Efficiency of single noise barriers*, Journal of Sound and Vibration, Vol. 146, 1991, pp. 303–322

[5] **Hothersall, D.C.**, **Crombie, D.H.**, **Chandler-Wilde, S.N.**: *The performance of T-profile and associated noise barriers*, Applied Acoustics, Vol. 32, 199, pp. 269–287

[6] **Baulac, M.**, **Defrance, J.**, **Philippe, J.**: *Optimisation with genetic algorithm of the acoustic performance of T-shaped noise barriers with a reactive top surface*, Applied Acoustics, Vol. 69, No. 4, 2008, pp. 332-342

[7] **Monazzam, M. R.**, **Lam, Y. W.**: *Performance of T-shape barriers with top surface covered with absorptive quadratic residue diffusers*, Applied Acoustics, Vol. 69, No. 2, 2008, pp. 93-109

[8] **Greiner, D.**, **Aznárez, J. J.**, **Maeso, O.**, **Winter, G.**: *Single- and multi-objective shape design of Y-noise barriers using evolutionary computation and boundary elements*, Advances in Engineering Software, Vol. 41, No. 2, 2010, pp. 368-378

[9] **Ishizuka, T.**, **Fujiwara, F.**: *Performance of noise barriers with various edge shapes and acoustical conditions*, Applied Acoustics, Vol. 65, No. 2, 2004, pp. 125-141

[10] **Crombie, D.H.**, **Hothersall, D.C.**: *The performance of multiple noise barriers*, Journal of Sound and Vibration, Vol.176, 1994, pp. 459–473

[11] **Martin, S. J.**, **Hothersall, D. C.**: *Numerical Modelling of Median Road Traffic Noise Barriers*, Journal of Sound and Vibration, Vol. 251, No. 4, 2001, pp. 671-681

[12] **Lim, C. W.**, **Cheong, C.**, **Shin, S.**, **Lee, S.**: *Time-domain numerical computation of noise reduction by diffraction and finite impedance of barriers*, Journal of Sound and Vibration, Vol. 268, 2003, pp. 385-401

[13] **Kinsler, L. E.**, **Frey, A. R.**, **Coppens, A. B.**, **Sanders, J. V.**; *Fundamentals of acoustics*, John Wiley and Sons

[14] **Jean, P.**, **Defrance, J.**, **Gabillet, Y.**: **The Importance of Source Type on the Assessment of Noise Barriers**, Journal of Sound and Vibration, Vol. 226, No. 2, 1999, pp. 201-216

[15] **Şteele, C.**: *A critical review of some traffic noise prediction models*, Applied Acoustics, Vol. 62, No. 3, 2001, pp. 271-287

[16] **Kirkup, S.**, **Yazdani, J.**: *A Gentle Introduction to the Boundary Element Method in Matlab/Freemat*, Academic Report: AR-08-14, The East Lancashire Institute of Higher Education at Blackburn College, Blackburn, 2008

[17] OPENBEM, *Open source Matlab codes for the Boundary Element Method*, http://www.openbem.dk, 2010

[18] CEN/TS 1793-3:1997, *Road traffic noise reducing devices - Test method for determining the acoustic performance - Part 3: Normalized traffic noise spectrum*

[19] **Štrumberger, N.**, **Viduka, K.**: *Traffic Impact on Environment Pollution in the First Decade of the 3rd Millennium*, Promet Traffic&Transportation, Vol. 13, 2001, pp. 119-124

[20] **Sviben, Z.**, **Toš, Z.**, **Borković, M.**: *Methods For an Acceptable Traffic Noise Level Design*, Promet Traffic&Transportation, Vol. 16, 2004, pp. 207-210